Powering Wireless Sensors using Magnetoelectric Wireless Power Transfer

Orpita Saha[1], Shad Roundy[2]

[1]Dept. of Electrical and Computer Engineering, University of Utah, Salt Lake City, UT 84112, USA

[2]Dept. of Mechanical Engineering, University of Utah, Salt Lake City, UT 84112, USA

E-mail: shad.roundy@utah.edu

***Abstract*—This paper presents a method to wirelessly power sensors using magnetoelectric (ME) structures as receivers. ME receivers consist of composites of magnetostrictive (MS) and piezoelectric material. Using ME receivers, as opposed to inductively coupled coils, is useful when a combination of small size and low frequency are desirable. Most ME receivers require a large DC magnetic field bias for high-performance operation. We present magnetization grading approach with multiple layers of MS material that results in high-performance structures with no DC magnetic field bias required. Our device produces 600 microwatts when excited by a 100 microtesla AC magnetic field at 192.3 kHz. The device is 12.4 mm X 5 mm X 1 mm. The corresponding normalized power density is 10.71 mWcm^{-3}Oe^{-2}, which is the highest reported to our knowledge.**

Keywords—Wireless power transfer, multiferroics, energy harvesting, magnetoelectric

I. Introduction

The number of wirelessly connected sensors has grown dramatically over the past two decades. This growth has driven research focused on powering such wireless devices. Broadly, power sources can be categorized as batteries, energy harvesting, or wireless power transfer (WPT). In reality, most sensors are, and will likely continue to be, powered by batteries. But, there are many applications in which batteries are not feasible, or at least have significant drawbacks. Fig. 1 shows how much power can be dissipated continuously from 1 cm^3 of battery volume versus time. Although chemistries differ, one cm^3 of battery volume can supply roughly 100 µW continuously for a year. Thus, alternative power sources, such as energy harvesting or WPT, make the most sense for applications in which replacement, or wired recharging, of a battery more often than about once per year is either infeasible or prohibitively expensive. Such cases include biomedical implants [1], [2], transportation infrastructure [3], manufacturing environments [4], and agricultural applications [5]. This paper focuses on WPT using magnetoelectric (ME) structures which are useful when a combination of low frequency and small size is important. This combination is valuable when transferring power through lossy media such human tissue, soil, or perhaps even water. In this paper, we will detail the design, modeling, and performance of ME composite structures used as receivers for WPT systems. In particular we will discuss the issue of a DC magnetic field bias and a method to overcome this bias resulting in high-performance, zero-bias, ME receivers.

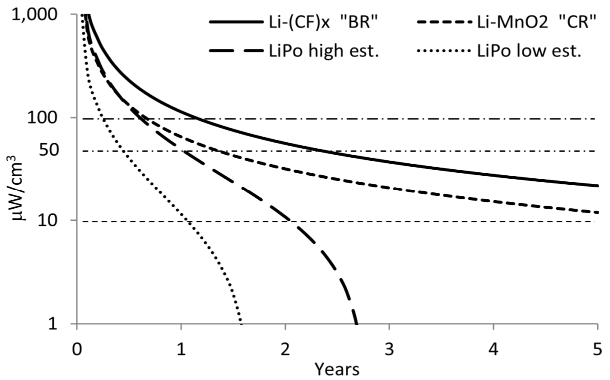

Fig. 1. Continuous power available per cm^3 of battery volume vs time for three battery chemitries. "BR" and "CR" types are primary batteries. LiPo high est. and LiPo low est. are the high and low estimates for lithium polymer rechargeable batteries. Internal leakage is taken into account.

II. Magnetoelectric Wireless Power Transfer

Near field WPT systems typically consist of inductively coupled coils, a transmitter and a receiver, in which the size of the coils is intimately tied to the operational frequency and distance between the coils. Thus, low frequency systems tend to be large. ME structures, however, offer much smaller receivers for a given frequency because their optimal operating frequency is defined by their acoustic, rather than electromagnetic, resonance. For example, a ME device of approximately 10 mm in length will operate at approximately 190 kHz which is orders of magnitude lower than a comparable inductively coupled WPT system. This frequency can be tuned with inductors and capacitors, however, the size of the components necessary is usually large by comparison to the ME structure itself.

ME structures directly couple the magnetic field to the electric field. Although single phase ME materials exist [6], almost all high performing devices are composites of magnetostrictive (MS) and piezoelectric material. In the receiver configuration (see Fig. 2), the MS material converts incoming magnetic fields to acoustic vibrations. The piezoelectric material converts the vibrations to an electric signal. Common MS materials include Terfenol-D, Galfenol, FeSiB (Metglas®), and nickel. Common piezoelectric materials include various formulations of lead zicronate titanate (PZT) and lead magnesium niobate-lead titanate (PMN-PT). The ME structure shown in Fig. 2 is known as a longitudinal mode oscillator and vibrates in extension mode along its length. We have developed models to optimize the design of ME receivers [7] and

2024 IEEE SENSORS | 979-8-3503-6351-7/24/$31.00 ©2024 IEEE | DOI: 10.1109/SENSORS60989.2024.10785003

shown that power levels on the order of 100 μW/mm^3 are possible from magnetic fields that are below the safety limit imposed by the IEEE safety standard [8], [9].

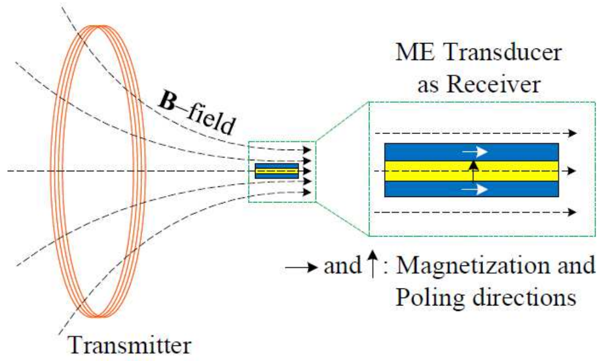

Fig. 2. Illustration of WPT system with coil transmitter and magnetoelectric (ME) receiver. The receiver is a composite of 3 layers. The top and bottom layers are magnetostrictive and are magnetized along their length. The middle layer is piezoelectric and is poled through its thickness. The structure vibrates longitudinally along its length [10].

III. Self-Biased ME WPT Structures

Truong [7] showed that the power output of a composite ME WPT receiver, such as that shown in Fig. 2, is proportional to the square of the piezomagnetic coefficient ($d_{33,m}$), which is a property of the MS material. The MS coefficient (λ) is defined as the strain resulting from an applied magnetic field H (i.e., $\lambda(H) = dl/l$ where l is the length of the material). The piezomagnetic coefficient is defined as $d_{33,m} = d\lambda/dH$. As shown in Fig. 3, the slope of the MS coefficient curve (value of $d_{33,m}$) reaches its maximum value at a non-zero magnetic field (H). Thus, for optimal performance, most MS materials require a DC magnetic field bias. This bias can be applied by permanent magnets or a nearby DC coil. However, either method can be problematic for many applications. Therefore, many self-biased, or zero-bias, approaches for ME composites have been explored [11], [12]. We have implemented a magnetization grading approach [13], [14] which removes the need for a DC bias field while still enabling high-performance operation.

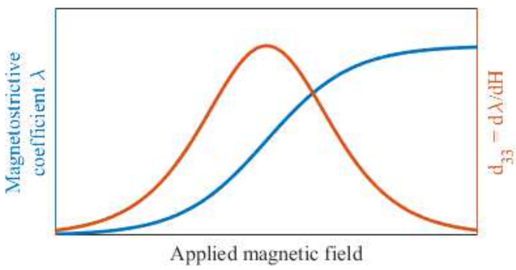

Fig. 3. Illustration of a typical curve for the magnetostrictive coefficient (λ) and piezomagnetic coefficient ($d_{33,m}$).

Grading in magnetization occurs when two dissimilar MS materials are laminated together. Due to the mismatch of saturation magnetizations (M_1, M_2) an internal field (H_{int}) is generated in the transverse direction, which is antiparallel to the grading of their magnetizations (∇M). This internal field attempts to align to the applied AC magnetic field (H_{ac}), creating an enhanced magnetostriction. Fig. 4 shows the magnetization grading principle.

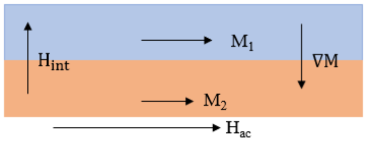

Fig. 4. Illustration of magnetization grading principle. Reproduced with permission from [13].

IV. Fabrication and Experimental procedure

A. Fabrication

We implemented a 5 layer device using Metglas and nickel as the two MS materials to create the magnetization grading and PZT-5A as the piezoelectric material (see Fig. 5). We diced 250 μm thick annealed pure (99.98%) nickel from Goodfellow Cambridge Limited, 23 μm thick Metglas® 2605SA1 (FeSiB) foils, and 500 μm thick PZT-5A sheets from Mide Technology according to the dimensions in Table I. We bonded the 5 layers with 105 West System epoxy resin and 206 hardener. The resulting laminates were cured at a temperature of 40 ºC for 5 hours under a hot press to remove access epoxy.

TABLE I. Average dimensions of the fabricated laminates.

Materials	Length, mm	Width, mm	Thickness, mm
PZT 5A	12.36	3.81	0.5
Nickel	10.16	5.00	0.25
Metglas	10.16	3.81	0.023

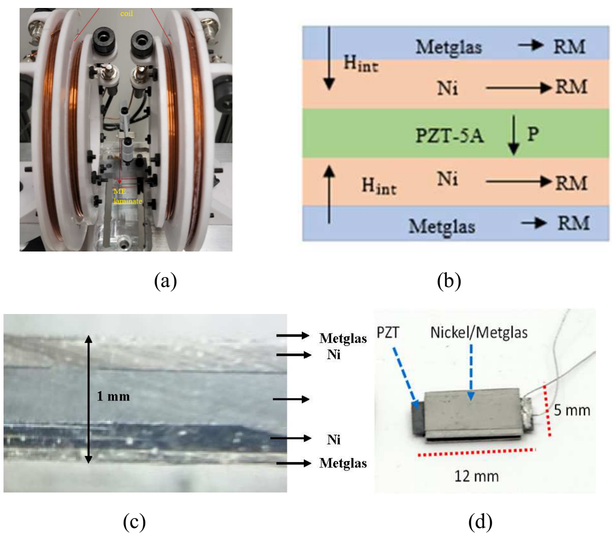

Fig. 5. (a) Helmholtz coil used to supply a uniform AC magnetic field, (b) schematic of device cross section, RM = remanent magnetization direction, P = polarization direction [13], (c) device cross section, (d) image of device. Figures (a) and (b) reproduced with permission from [13]

B. Experimental Procedure

We pre-magnetized the laminates with a field of approximately 90 mT, reducing the field to zero slowly.

The authors would like to acknowledge support for this research from the National Science Foundation under award number: 1651438.

After pre-magnetization, the ME device was placed in a Helmholtz coil (see Fig. 5(a)) to apply the AC magnetic field of 100 μT AC RMS. The frequency of the applied AC magnetic field was swept to create a frequency response curve and identify the resonance frequency. Power at the resonance frequency was measured for a range of load resistances. We discussed the experimental process in more detail in our prior work [13].

V. Results and discussion

A. Self-biased 5 layer laminate performance analysis

Fig. 6 shows the frequency response of 5 symmetric 5-layer self-biased ME laminates (D0, D1, D2, D3, D4). Fig. 7 shows the power output of the same laminates versus load resistance. The optimum load is around 4 kΩ. Table II summarizes the maximum peak-to-peak voltages and power output.

TABLE II. Peak-to-peak voltage and power output for 5 self biased ME receivers.

	D0	D1	D2	D3	D4
Vpp, volts	7.43	6.77	6.43	6.46	6.26
Power, μW	326	320	293	298	297

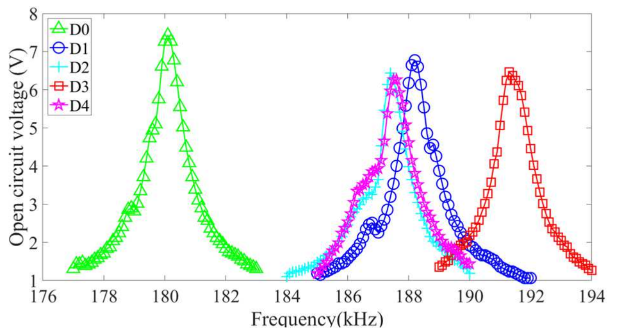

Fig. 6. Frequency response of self-biased ME laminates. Applied AC magnetic field is 100 μT. Reproduced with permission from [13]

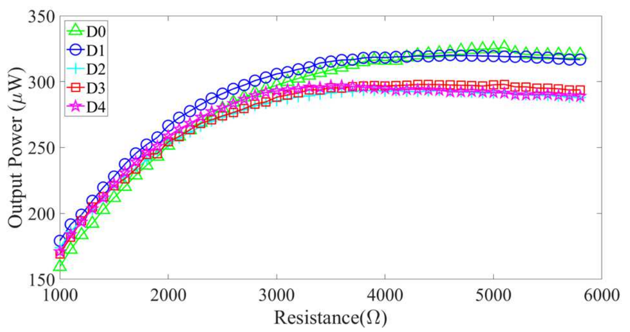

Fig. 7. Self-biased ME laminates power output at resonance versus resistance. Applied AC magnetic field is 100 μT. Reproduced with permission from [13].

B. Power versus metglas thickness

The high permeability Metglas layer is very thin by comparison to the adjacent nickel layer. We conducted experiments to investigate the effect of adding more Metglas layers hypothesizing that thicker Metglas would create a higher H_{int} and an enhanced magnetostriction effect. Fig. 8 shows the power output for a 100 μT RMS AC field supply at resonance (192.3 kHz) and optimal load resistance (4 kΩ) as a function of the number of Metglas layers. (Note, each layer is 23 μm thick.) The 3-layer device performed the best exhibiting a power output of 600 μW.

Power scales with the volume of the device and the square of the magnetic field [15], thus it is useful to normalize power output by these two parameters. However, even using normalized power density, it is challenging to compare the power output of our self-biased devices with other self-biased devices in the literature because most are characterized only as sensors (i.e., open circuit voltages are reported, but not device impedance or power output). However, we can compare our self-biased device with devices that use permanent magnets or coils to provide a DC bias. A comprehensive comparison of such devices can be found in [15]. The highest normalized power density that we have found is 7.4 $mWcm^{-3}Oe^{-2}$, reported by Wang *et. al.* [16]. Their device is an externally biased ME laminate composed of Terfenol-D and PMN-PT. From Fig. 8, the devices with one and three layers of Metglas exhibit normalized power densities of 6.14 $mWcm^{-3}Oe^{-2}$ and 10.71 $mWcm^{-3}Oe^{-2}$, respectively. Thus, our self-biased WPT receivers match, and even exceed, the DC biased devices reported in the literature.

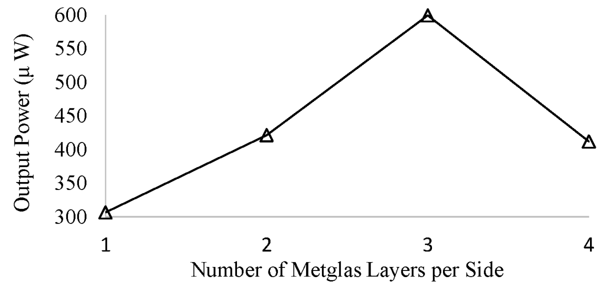

Fig. 8. Output power of ME laminates at 100 μT RMS AC field supply versus number of metglas layers per side.

As the number of Metglas layers increases, the grading effect and power output are both enhanced up to three layers (72 μm). Beyond three layers, the power falls indicating an optimum for the ratio of Metglas/nickel thickness. Possible reasons include: increased adhesive layers that increase both mass and damping, increased “dead” mass from the Metglas far away from the Metglas/nickel interface, and increased demagnetizing effect. The exact nature of this optimum for magnetization graded ME devices needs further exploration.

VI. Conclusion

In this paper, we introduced ME receivers for WPT systems in the context of powering wireless sensors. This approach is particularly useful where a combination of low frequency and small size is desirable. We have demonstrated self-biased ME receivers using a magnetization grading effect that results from the mismatch in saturation magnetization at the Metglas/nickel interface. The best performing ME receiver design, with 3-layers of Metglas exhibits a normalized power density of 10.71 $mWcm^{-3}Oe^{-2}$, which exceeds the best reports normalized power density for ME WPT receivers, including those with a DC magnetic field bias.

VII. References

[1] D. B. Ahire, "Wireless power transfer system for biomedical application: A review," *International Conference on Trends in Electronics and Informatics (ICEI)*, Tirunelveli, India, pp. 135–140, 2017, doi: 10.1109/ICOEI.2017.8300903.

[2] E. Andersen, O. Saha, and S. Roundy, "A Dynamic Transmit Coil for Wirelessly Powering Small ME Transducer based Biomedical Implants," *2021 IEEE 20th International Conference on Micro and Nanotechnology for Power Generation and Energy Conversion Applications, PowerMEMS 2021*, vol. 2, no. December, pp. 212–215, 2021, doi: 10.1109/PowerMEMS54003.2021.9658362.

[3] S. Li and C. C. Mi, "Wireless power transfer for electric vehicle applications," *IEEE J Emerg Sel Top Power Electron*, vol. 3, no. 1, pp. 4–17, 2015, doi: 10.1109/JESTPE.2014.2319453.

[4] J. Van Mulders *et al.*, "Wireless Power Transfer: Systems, Circuits, Standards, and Use Cases," *Sensors*, vol. 22, no. 15, 2022, doi: 10.3390/s22155573.

[5] A. M. Jawad, H. M. Jawad, R. Nordin, S. K. Gharghan, N. F. Abdullah, and M. J. Abu-Alshaeer, "Wireless power transfer with magnetic resonator coupling and sleep/active strategy for a drone charging station in smart agriculture," *IEEE Access*, vol. 7, pp. 139839–139851, 2019, doi: 10.1109/ACCESS.2019.2943120.

[6] H. Palneedi, V. Annapureddy, S. Priya, and J. Ryu, "Status and perspectives of multiferroic magnetoelectric composite materials and applications," *Actuators*, vol. 5, no. 1. MDPI AG, Mar. 01, 2016. doi: 10.3390/act5010009.

[7] B. D. Truong and S. Roundy, "Experimentally validated model and power optimization of a magnetoelectric wireless power transfer system in free-free configuration," *Smart Mater Struct*, vol. 29, no. 8, Aug. 2020, doi: 10.1088/1361-665X/ab90a2.

[8] W. H. Bailey *et al.*, *Synopsis of IEEE Std C95.1™-2019 "IEEE Standard for Safety Levels with Respect to Human Exposure to Electric, Magnetic, and Electromagnetic Fields, 0 Hz to 300 GHz,"* vol. 7. 2019. doi: 10.1109/ACCESS.2019.2954823.

[9] B. D. Truong, "Wireless Power Transfer for Wearable and Implantable Medical Devices," PhD dissertation, University of Utah, Salt Lake City, 2021.

[10] E. J. Andersen, "Wireless Power Transfer to mm-Scale Biomedical Implants," PhD dissertation, University of Utah, Salt Lake City, 2022.

[11] V. Annapureddy *et al.*, "Magnetic energy harvesting with magnetoelectrics: An emerging technology for self-powered autonomous systems," *Sustain Energy Fuels*, vol. 1, no. 10, pp. 2039–2052, 2017, doi: 10.1039/c7se00403f.

[12] O. Saha, E. Andersen, and S. Roundy, "Wireless Power Transfer by Self-biased Magnetoelectric Laminate for Biomedical Implants," *2021 IEEE 20th International Conference on Micro and Nanotechnology for Power Generation and Energy Conversion Applications, PowerMEMS 2021*, no. December, pp. 36–39, 2021, doi: 10.1109/PowerMEMS54003.2021.9658356.

[13] O. Saha, E. Andersen, and S. Roundy, "A self-biased magnetoelectric wireless power transfer receiver targeting biomedical implants," *Sens Actuators A Phys*, vol. 360, no. July, p. 114558, 2023, doi: 10.1016/j.sna.2023.114558.

[14] E. Andersen, O. Saha, and S. Roundy, "System Demonstration and Characterization of a Self-Biased Magnetoelectric Wireless Power Transfer System for Biomedical Implants," *2022 21st International Conference on Micro and Nanotechnology for Power Generation and Energy Conversion Applications, PowerMEMS 2022*, no. December, pp. 94–97, 2022, doi: 10.1109/PowerMEMS56853.2022.10007081.

[15] O. Saha, B. D. Truong, and S. Roundy, "A review of wireless power transfer using magnetoelectric structures," *Smart Mater Struct*, vol. 31, no. 11, 2022, doi: 10.1088/1361-665X/ac9166.

[16] Y. Wang *et al.*, "Electrical resistance load effect on magnetoelectric coupling of magnetostrictive/piezoelectric laminated composite," *J Alloys Compd*, vol. 500, no. 2, pp. 224–226, 2010, doi: 10.1016/j.jallcom.2010.04.009.